



A Numerical Investigation of the Flow Regime and Flow Direction on the Heat Transfer Performance and Pressure Drop of a Double Pipe Heat Exchanger

Shahed Alrawashdeh^{1*}, Dana Alshamaileh², Mohammad Qasem²

¹ Marine Science Department, Aqaba University College, AL-Balqa Applied University (BAU), As-Salt 77110, Jordan

² Mechanical Engineering Department, AL-Balqa Applied University (BAU), As-Salt 19110, Jordan

Corresponding Author Email: shahed.rawashdeh.27@bau.edu.jo

Copyright: ©2026 The authors. This article is published by IETA and is licensed under the CC BY 4.0 license (<http://creativecommons.org/licenses/by/4.0/>).

<https://doi.org/10.18280/ijht.440124>

ABSTRACT

Received: 21 December 2025

Revised: 15 February 2026

Accepted: 23 February 2026

Available online: 28 February 2026

Keywords:

heat exchanger, heat transfer, logarithmic mean temperature difference, computational fluid dynamics, pressure drop, Re number

In this study, computational fluid dynamics simulations were conducted to investigate the combined influence of flow regime and flow direction on the thermo-hydraulic performance of a double-pipe heat exchanger. The laminar, transitional, and turbulent flow regimes were simulated using two-dimensional models with Reynolds numbers of 1500, 3000, and 6000, respectively. For both parallel flow and counter flow configurations, the influence of the Reynolds number on the pressure drop and heat transfer rate was examined. It is clear that while a lower Reynolds number results in lower heat transfer rates with minimal pressure drop, a higher Reynolds number results in improved heat transfer rates at the expense of higher pressure drop. Compared to the parallel flow configuration, the counter flow configuration is more effective in terms of heat transfer with a higher logarithmic mean temperature difference and a slight increase in pressure drop. Counter-flow in the transitional flow regime offers the best compromise between power consumption and heat transfer enhancement among all the considered cases.

1. INTRODUCTION

Heat exchangers (HEs) are crucial in various industries and engineering systems, including power production, transportation, HVAC, and refrigeration, improving heat transfer between fluids [1-3]. Their performance depends on several factors, such as heat transfer mechanism, fluid flow direction, and structural design [4-6]. Among the various HE types, including shell and pipe, plate, double pipe, and finned pipe, the double pipe HE is widely used in the engineering sector because of its simple design, pipe inside a pipe maintenance, disassembly, assembly, and its applicability to almost all cooling and heating applications [3, 7-11]. These HEs are configured into two main types: counter and parallel flow [12, 13]. In a parallel flow HE, a rapid decrease in the temperature difference between the hot and cold fluids over its length occurs since the fluid inlets are in the same direction [14]. In contrast, a counter-flow HE maintains a higher temperature gradient due to the opposite direction of the two fluids' motion. Thus, compared with parallel flow designs, counter flow designs are generally more effective in heat transfer [3, 13].

HEs are typically constructed from materials with high thermal conductivity and excellent corrosion resistance, such as copper and aluminum, as these materials endure corrosion while providing superior thermal conductivity [15].

The hydraulic and thermal performance of HEs has become of paramount importance in waste energy minimization in power systems and industrial and engineering processes [5, 16, 17]. Thus, a less than optimal design of the HE or conditions

of flow that are less than optimal normally lead to huge losses of energy, with reduced thermal and mechanical efficiency; optimization, therefore, remains imperative [18, 19]. Previous studies have shown that non-uniform flow distribution deteriorates thermal performance by reducing heat transfer coefficients and increasing thermal resistance, Zhang et al. [20] conducted a quantitative study to assess uneven flow distribution on thermal performance, and it was found that poor flow led to a deterioration in the thermal performance (heat transfer coefficient, capacity, and increased thermal resistance) of HE. Furthermore, highly efficient HEs control system reliability and stability by conserving thermal energy without loss, maintaining necessary temperatures, and increasing overall productivity [5, 21-25].

The main thermal and mechanical characteristics of a double pipe HE are determined by various parameters, including HE design, convection heat transfer coefficient, pressure drop, and temperature distribution, all of which depend on the mass flow rate of the working fluid. After conducting an experimental investigation of a double pipe HE at different flow rates and flow directions. Furthermore, increasing the flow rate between hot and cold streams improves the thermal efficiency, especially in counterflow systems [26, 27].

The flow rate is directly related to a dimensionless value known as the Reynolds (Re) number. This number is used in fluid mechanics to predict the nature of the flow, indicating whether the flow is laminar, turbulent, or transitional inside the inner tube and annulus [28, 29]. In laminar flow, Re numbers are low, resulting in a smooth and orderly fluid flow,

leading to limited mixing and the formation of thicker thermal boundary layers [30-33]. As the Reynolds number increases, turbulent flow develops, characterized by chaotic et al. fluid motion, enhanced mixing, and disruption of boundary layers, with distinct behavioral differences between the two regimes [30, 34-37]. Between these two types lies a transitional flow pattern, occurring within a specific range of Re numbers, exhibiting a combination of laminar and turbulent characteristics [28, 36]. In this type, even minor turbulence can lead to localized disturbances, causing fluctuations in temperature and flow velocity. Thus, understanding the trade-off between thermal enhancement and flow regime is fundamental to optimal HE design for high thermal efficiency with minimum energy consumption [38-40].

Apart from concentrating on the flow system and direction, other researchers have resorted to the development of new technologies that can enhance heat transfer in heat HEs. Some of the new technologies that have been developed include the use of fluids with certain properties, such as nanofluids, and the enhancement of the heat transfer surface area through the use of extended surfaces such as fins, spiral tubes, and internal gaskets [41, 42]. Choi et al. [43] reported that using nanofluids in HEs increases the heat transfer coefficient due to their high thermal conductivity, particularly metal oxide nanofluids. However, despite this improvement, increasing the viscosity of the nanofluids can lead to a significant pressure drop, reflecting a conflict between thermal and hydraulic performance [44]. Also, in an experimental study conducted by Sivalakshmi et al. [45] on a double tube heat exchanger with helical fins, the heat transfer rate was shown to be increased compared to a tube without any additives. The heat transfer coefficient increased by up to 35%.

Although these technologies have been successful in improving heat transfer rates, they have been linked with difficulties such as increased pressure drops, operating costs, and design complexities [46].

Recently, most researchers have turned to numerical analysis and simulation software to study flow types and their impact on the mechanical and thermal performance of HEs [47]. For example, many engineering phenomena can be predicted using computational fluid dynamics (CFD), yielding results such as velocity patterns, temperature distribution, and local heat transfer characteristics using finite-volume (FVM) techniques without the need for laboratory equipment or time [48]. This method allows for the numerical partitioning and solution of the governing equations of energy, momentum, and mass, providing valuable insights into heat exchanger performance. Kotian et al. [49] conducted a numerical analysis to elucidate the effect of coolant flow rates within a HE on the temperature distribution during the cooling process, and Banu et al. [50] demonstrated the effect of coolant or heating mass flow rates on heat transfer rates in HEs using CFD modeling, employing variable inputs such as mass flow rate, inlet temperatures, and specific heat. Debtera et al. [51] conducted direct comparisons of different mass flow combinations in double pipe HEs using CFD, and the results showed trends in the mean logarithmic temperature difference (LMTD), efficiency, and coefficient of friction with different flow rates. Hassan and Abdulmajeed [52] determined that increasing the mass flow rate enhances overall heat transfer and thermal efficiency, based on a CFD study conducted at different mass flow rates.

In general, previous research in CFD has provided important insights into how mass flow rate affects HE

efficiency. However, there appears to be a scarcity of research that has attempted to investigate the integral effect of both flow regimes and HE flow patterns. More specifically, the mutual relationship concerning flow patterns (laminar flow, turbulent flow), HE patterns (Parallel flow HE, Counter flow HE), alongside key thermodynamic factors such as temperature distribution, heat flux, and pressure drop.

In this study, the Re number was deliberately chosen as the primary dimensionless indicator to represent changes in mass flow rate, facilitating a systematic study of the effects of the flow system under comparable dynamic conditions. Unlike traditional studies that evaluate thermal or hydraulic performance separately, this study establishes an integrated system combining thermal and hydraulic aspects. CFD analysis is used to simultaneously assess the flow types impact through three key performance indicators: temperature distribution, heat transfer rate, and pressure drop, comparing parallel flow HE and counter flow HE under identical geometrical and boundary conditions. A better understanding of how the flow system and HE design work together to improve thermal performance and lower friction is made possible by this integrated and comparative approach.

2. METHODS

A double pipe HE is a heat exchange where two fluids flow inside the concentric tubes. Its operation is basically driven by convection and conduction, which then determine the heat transfer rate and the required pumping force. The pressure drop and LMTD are key parameters in the assessment of thermal and hydraulic performance. Either laminar or turbulent fluid flow would significantly influence both parameters.

2.1 Reynolds number and flow regimes

The Re number is the fundamental dimensionless quantity used to recognize whether flow is laminar, turbulent, or transitional. It is defined as:

$$Re = \frac{\rho u D_h}{\mu} \quad (1)$$

Based on its value, when $Re < 2300$, the flow is considered Laminar. However, when $2300 < Re < 4000$, the flow is transitional and turbulent when $Re > 4000$. The flow regime directly affects heat transfer coefficients, temperature distribution, and ultimately pressure drop, heat transfer rate, and LMTD [53].

2.2 Reynolds number and pressure drop

The pressure drop represents the resistance encountered by the fluid as it flows through the inner tube and outer channel of the HE. It is described by the Darcy-Weisbach equation [53]:

$$\Delta P = f \frac{L}{D_h} \frac{\rho u^2}{2} \quad (2)$$

Laminar flow:

$$f = Re (64)^{-1} \quad (3)$$

Turbulent flow:

$$f = 0.316 (\text{Re})^{-0.25} \quad (4)$$

2.3 Heat transfer for double pipe HEs using mean logarithmic temperature difference

The rate of heat transfer in a double pipe HE is controlled by the LMTD, which describes how effective the heat flow is between the two fluids. The overall heat transfer is described through Eq. (5) below [53].

$$Q = U A \Delta T_{LM} \quad (5)$$

where, U is the overall heat transfer coefficient, and A is the area of heat transfer. The LMTD is an insulation for the non-uniform variation of temperature. One important measure of HE performance is the LMTD. Along the counter and parallel flow, HE takes into account the temperature differential between hot and cold fluids. As shown in Figure 1.

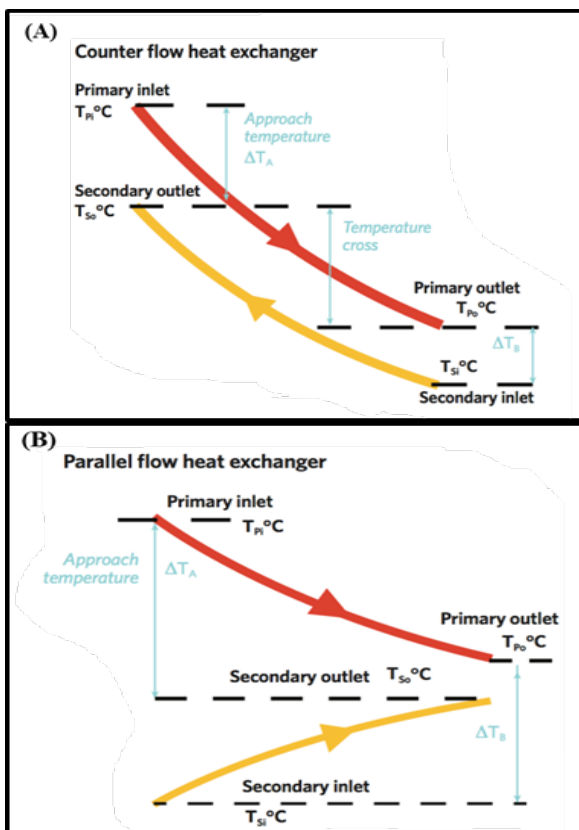


Figure 1. Temperature distribution for (a) A counter flow HE; (b) A parallel flow HE [54]

The following formula represents the LMTD in parallel flow HE, and counter flow HE:

$$\Delta T_{LM} = \frac{\Delta T_2 - \Delta T_1}{\ln\left(\frac{\Delta T_2}{\Delta T_1}\right)} \quad (6)$$

Therefore:

$$\Delta T_1 = T_{h,1} - T_{c,1} \quad (7)$$

$$\Delta T_2 = T_{h,2} - T_{c,2} \quad (8)$$

For parallel flow HE, it flows that:

$$T_{h,1} = T_{h,i}, \quad T_{h,2} = T_{h,o}, \quad T_{c,1} = T_{c,i}, \quad T_{c,2} = T_{c,o}.$$

For counter flow HE, it flows that:

$$T_{h,1} = T_{h,i}, \quad T_{h,2} = T_{h,o}, \quad T_{c,2} = T_{c,i}, \quad T_{c,1} = T_{c,o}.$$

3. COMPUTATIONAL FLUID DYNAMICS METHODOLOGY

The basis of this research is to evaluate the effect of laminar, turbulent, and transitional flow types using varying mass flow rates and Re numbers within a CFD model to determine the optimal mass flow rate. A comparison is then conducted between the effects of different flow types on the thermal efficiency of HE. Figure 2 illustrates the CFD analysis methodology.

3.1 Geometry modeling

The 2D geometry of the HE domain was constructed through the built-in design module in ANSYS Workbench 2020. The HE is composed of an outer copper pipe with a diameter of 0.05 m, inside which is another copper tube with a diameter of 0.025 m and a length of 1 meter, as shown in Figure 3.

3.2 Mesh generation

A rectangular mesh element was adopted to discretize the HE domain with a size of 5×10^{-4} m, as shown in Figure 4. Also, a refinement is applied at the interface between the inner and outer pipes. The convergence of the difference in temperature between the inner and outer of both streams was reported to determine the number of elements.

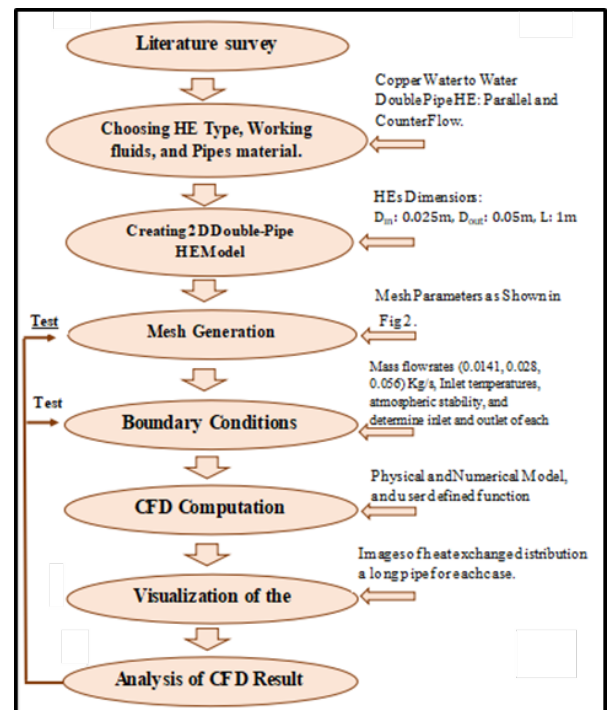


Figure 2. The CFD methodology

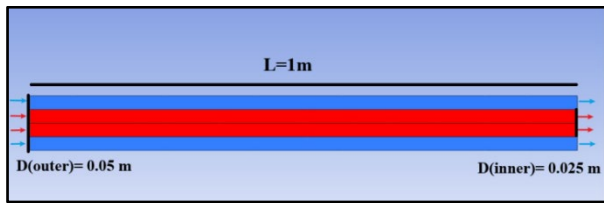


Figure 3. 2D HE geometry model

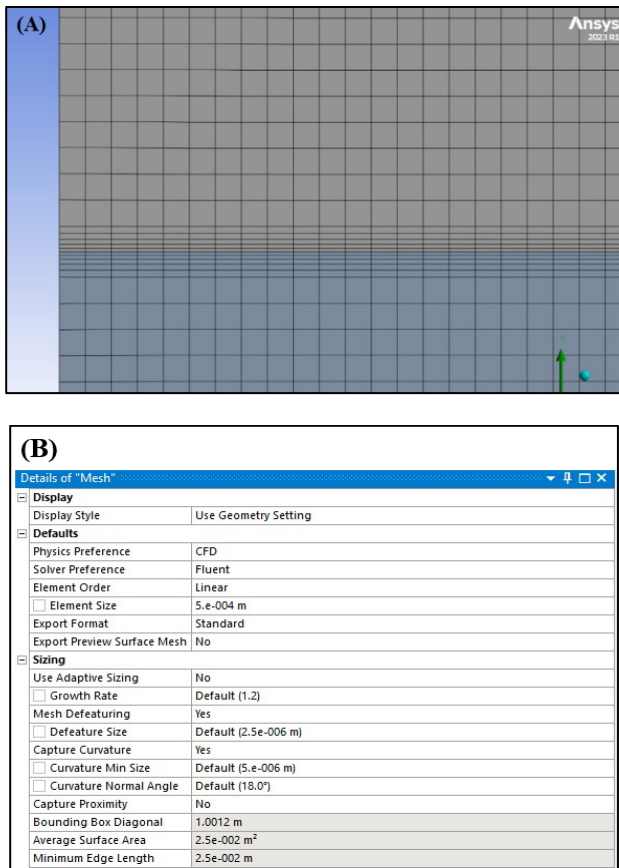


Figure 4. (A) The created mesh with inflation at the interface; (B) Mesh metrics details

4. BOUNDARY CONDITIONS

The inlet and the outlet boundary conditions of each case are shown in Table 1. An ambience pressure boundary condition was applied at the outlets for both the inner and outer streams

Table 1. Inlet boundary conditions

	Hot Fluid Side	Cold Fluid Side
Case (1): Laminar flow		
	Inner Flow	Outer Flow
Flow rate value (Kg/s)	14.1×10^{-3}	14.1×10^{-3}
Inlet temperature (K)	353.15	293.15
Case (2): Transitional flow		
	Inner Flow	Outer Flow
Flow rate value (Kg/s)	28×10^{-3}	28×10^{-3}
Inlet temperature (K)	353.15	293.15
Case (3): Turbulent flow		
	Inner Flow	Outer Flow
Flow rate value (Kg/s)	56×10^{-3}	56×10^{-3}
Inlet temperature (K)	353.15	293.15

5. RESULTS AND DISCUSSIONS

In this section, the flow regimes will be investigated based on two key performance parameters of a parallel flow HE and a counter flow HE, namely LMTD and pressure drop. The results include an analysis of three operating conditions with varying Re numbers of 1500, 3000, and 6000, representing laminar, transitional, and turbulent flow conditions, respectively. The inlet temperatures of both hot and cold streams are maintained at 353.15 K and 293.15 K, respectively, while the inlet mass flow rate is adjusted to achieve the required flow regime.

5.1 Heat transfer characteristics in a parallel flow double-pipe HE

The results generally show that in a parallel flow HE, the temperature difference between cold and hot water is greatest at the inlet because both enter from the same end. Then the difference gradually decreases along the length of the HE pipe. Under laminar flow condition (Re = 1500, mass flow rate = 0.0141 kg/s) for both fluids, exhibits a gradual change in the average axial temperature, leading to a rapid decrease in the temperature difference at the inlet and a decrease in the heat transfer area along the flow direction of the HE, as shown in Figure 5(a), this is due to poor mixing and increased thermal boundary layer thickness. Consequently, the heat transfer capacity is limited to 560 W, accompanied by a relatively low LMTD value, indicating weak overall thermal performance.

When the flow transitions to a transition flow regime (Re = 3000, mass flow rate = 0.028 kg/s), the temperature gradients become steeper compared to laminar flow, as shown in Figure 5(b). Consequently, heat transfer improves to 905.5 W, which represents an increase of approximately 62% compared to the laminar regime, due to flow instability and increased thermal mixing.

When the flow transitions to a turbulent flow regime (Re = 6000, mass flow rate = 0.056 kg/s), the temperature gradients at the outlet between the hot and cold water become more homogeneous and closely matched, as shown in Figure 5(c). This is due to strong thermal mixing and a significant decrease in the thermal boundary layer thickness. Consequently, the heat transfer efficiency improves to about 1600 W, corresponding to an increase of about 185% relative to laminar flow and 77% compared to transitional flow, resulting in better thermal performance.

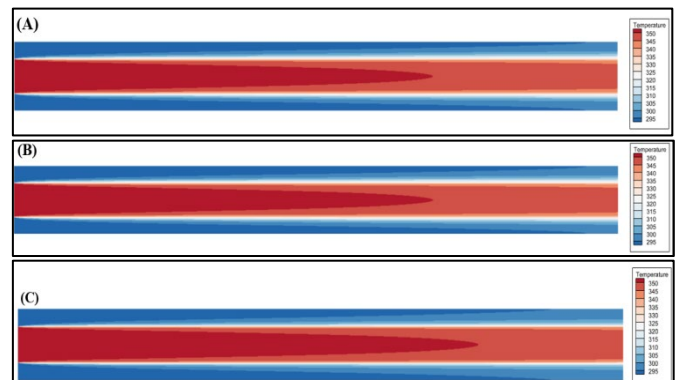


Figure 5. Parallel flow HE temperature distribution for (A) Laminar flow, (B) Transitional, and (C) Turbulent

Despite this improvement, the parallel flow configuration still exhibits a decrease in temperature driving force. Figure 6 shows the improvement in heat transfer rate in a parallel flow HE with increasing Re number and mass flow rate. A comprehensive list of thermal performance metrics for the three flow regimes of a parallel flow HE can be found in Table 2.

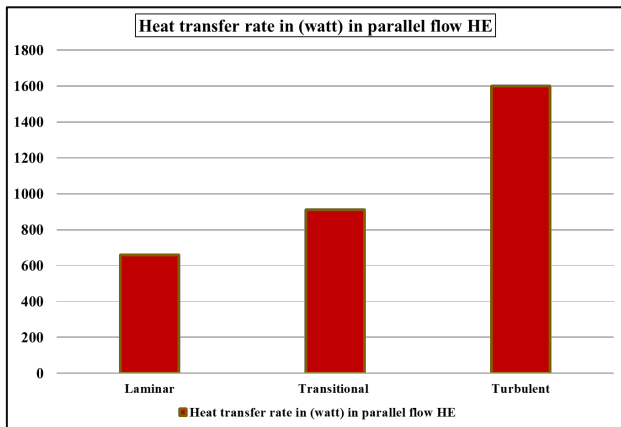


Figure 6. The parallel flow HE heat transfer rate for different flow regimes

Table 2. Thermal performance metrics for the three flow regimes of a parallel flow HE

Flow Regimes	Re Number	Heat Transfer Rate (Watts)	LMTD (K)
Laminar	1500	560	47
Transition	3000	905.5	49
Turbulent	6000	1600	51

5.2 Heat transfer characteristics in a counter flow HE

In the case of laminar flow ($Re = 1500$, mass flow rate = 0.0141 kg/s), a counter flow HE realizes a greater length-wise temperature difference (LMTD) than a parallel flow HE, as indicated in Figure 7(a). Though the heat transfer rate is restricted by the nature of laminar transport, a better thermal use of the exchange surface is attained in the case of counter flow heat transfer, resulting in a heat transfer rate of 592 W.

In the case of transitional flow with ($Re = 3000$, mass flow rate = 0.028 kg/s), the CFD solution indicates a greater reduction in the outlet temperature difference than in parallel flow, as indicated in Figure 7(b). Therefore, heat transfer rates are appreciably enhanced owing to greater mixing of the fluid and turbulence in the boundary layer. Simultaneously, the latter allows an entire span of the HE to profit from the increase in heat transfer rates to about 942 W, indicating a roughly 59.5% improvement over the laminar regime.

The final case involving turbulent flow with ($Re = 6000$, mass flow rate = 0.056 kg/s), in which the HE is in the opposite direction, reveals the maximum heat transfer rate of 1644 W, representing a further increase of approximately 74.5% relative to the transitional flow. The CFD solution reveals a great deal of mixing of the fluid, a strong temperature gradient as indicated in Figure 7(c), and a uniform axial force function in the HE. The values of (LMTD) calculated in this case are appreciably greater than in parallel flow conditions. Figure 8 shows the improvement in heat transfer rate in a counter flow HE with increasing Re number and mass flow rate. A comprehensive list of thermal performance metrics for the

three flow regimes of a counter flow HE can be found in Table 3.

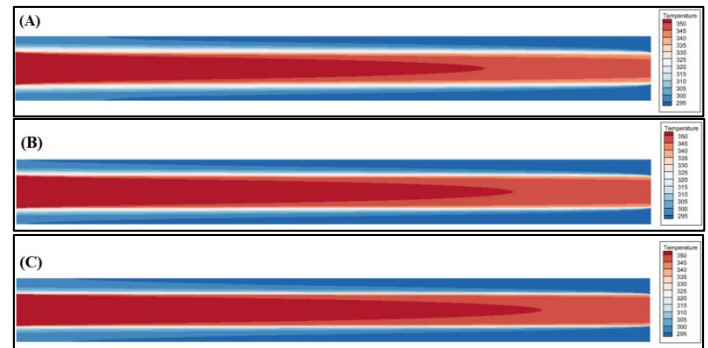


Figure 7. Counter flow HE temperature distribution for (A) Laminar flow, (B) Transitional, and (C) Turbulent

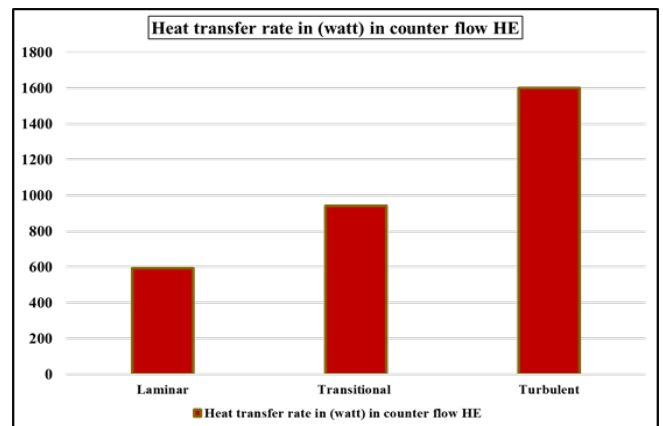


Figure 8. The counter flow HE heat transfer rate for different flow regimes

Table 3. Thermal performance metrics for the three flow regimes of a counter flow HE

Flow Regimes	Re Number	Heat transfer rate (Watt)	LMTD (K)
Laminar	1500	592	48.5
Transition	3000	942	50.7
Turbulent	6000	1644	52

5.3 Pressure drop characteristics in counter flow HE, and parallel flow HE

The CFD pressure line analysis demonstrates that both configurations of HE exhibit nearly identical pressure drop behavior under the same operating conditions, indicating that pressure losses are predominantly governed by the flow regime and mass flow rate rather than the flow arrangement. Under laminar flow conditions, where the mass flow rate is 0.0141 kg/s, the pressure drop is minimal, approximately 0.1462 Pa and 0.0502 Pa for the inner and the outer pipe, respectively, due to low velocity gradients and low wall shear stress. However, with transitional flow, where the mass flow rate is 0.028 kg/s, the pressure drop increases non-linearly to 0.3873 Pa for the inner pipe, and 0.1081 Pa for the outer pipe with increasing turbulence, thermal mixing, evolving velocity gradients, and increasing shear stress. After increasing the mass flow rate to 0.056 kg/s, where the flow is turbulent, the pressure drop increases significantly to 1.1226 Pa for the inner pipe and 0.2570 Pa for the outer pipe due to increased shear

stress and momentum exchange. These results confirm that, for both parallel flow HE and counter flow HE, the pressure drop increases substantially with increasing mass flow rate and turbulence intensity, while the influence of flow direction on pressure losses remains negligible.

Figure 9 shows the pressure drop in both the inner and outer tubes for all three flow conditions. The inner tube always has a higher pressure drop than the outer tube. This is because the inner tube has a smaller hydraulic diameter.

The corresponding velocity profiles in the axial direction, as shown in Figure 10 for the parallel flow and counter flow arrangements, respectively, further support the above conclusions. The smooth velocity profiles for the laminar flow and the higher velocity gradients near the walls for the transitioning flows from laminar to turbulent can be used to explain the increase in pressure losses.

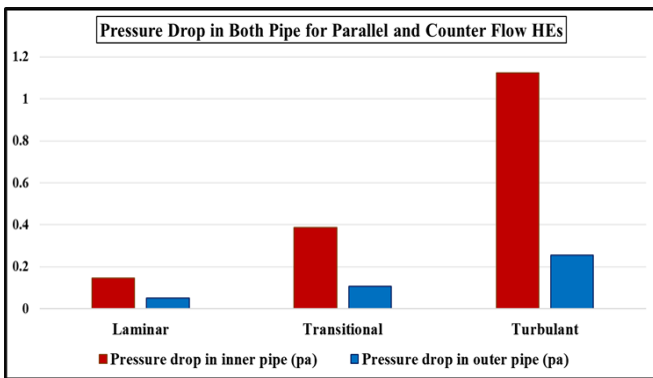


Figure 9. Pressure drop for different flow regimes in parallel and counter flow HEs

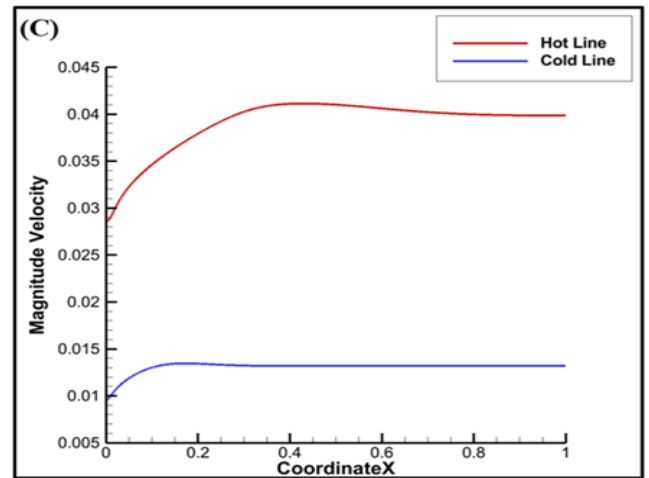
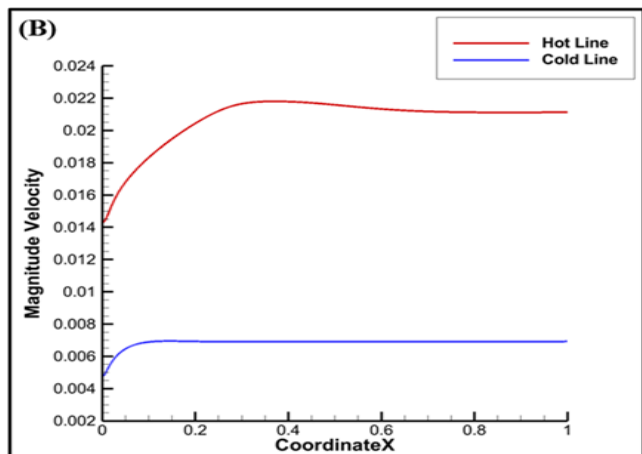
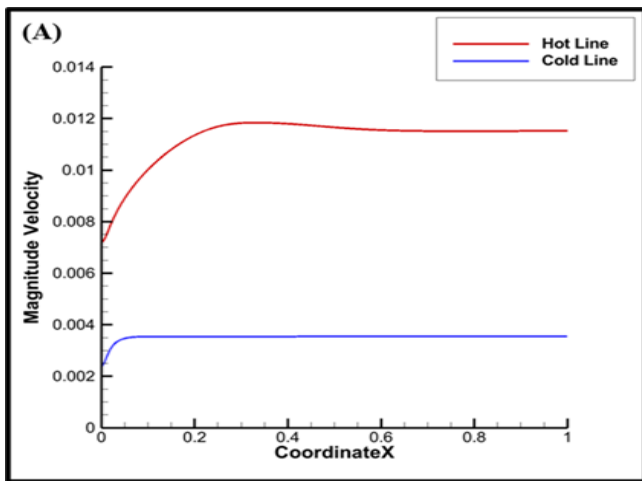


Figure 10. Parallel and counter flow HE temperature distribution for (A) Laminar flow, (B) Transitional, and (C) Turbulent

5.3 Comparison between parallel and counter flow HEs

CFD simulation results comparing parallel and counter flow designs show that the thermal performance of counter flow HEs surpasses that of parallel flow in all flow regimes. The counter flow design achieves higher overall values for both the (LMTD) and heat transfer rates. This advantage becomes more pronounced with increasing Re numbers. However, despite the higher heat transfer rates, the pressure drop along the HE for both tubes is the same for both parallel and counter flow designs in all flow regimes. This is because the pressure drop is primarily affected by the flow regime rather than its direction. Figure 11 illustrates the heat transfer rate for both parallel flow HE and counter flow HE for all regimes.

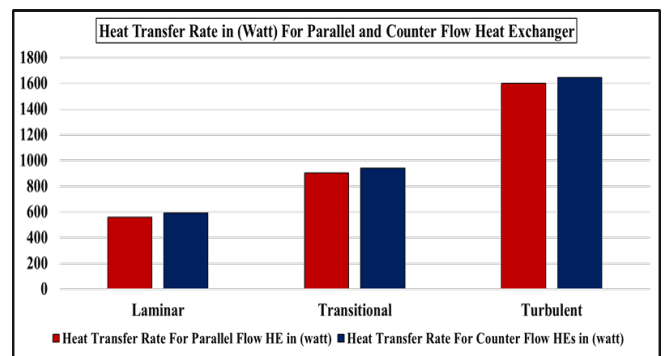


Figure 11. Heat transfer rate comparison between parallel flow HE and counter flow HE

6. CONCLUSIONS

CFD analysis shows that the heat transfer rate rises with the Reynolds number because of increased mixing in the flow, resulting in a substantial pressure drop. The laminar flow results in the lowest pressure drop but poor heat transfer rates, while the turbulent flow results in higher heat transfer rates at the cost of higher pressure drops. Based on the operating conditions and geometry chosen for this study, the transitional flow results in balanced heat transfer and pressure drop. Additionally, the counterflow HE performs better than the parallel flow HE for both heat transfer rates and LMTD. These

results are valid for the range of parameters studied in this work.

Future research should broaden the analysis to include more geometric variations, different working fluids, and wider ranges of Reynolds numbers. It should also include experimental validation to improve how the findings can be applied in general.

REFERENCES

- [1] Hesselgreaves, J.E., Law, R., Reay, D. (2016). Compact Heat Exchangers: Selection, Design and Operation. Butterworth-Heinemann. <https://books.google.at/books?id=je8QCgAAQBAJ>.
- [2] Shah, R., Sekulic, D. (1998). Heat Exchangers. McGraw-Hill.
- [3] Bell, K.J. (2004). Heat exchanger design for the process industries. *Journal of Heat Transfer*, 126: 877-885. <https://doi.org/10.1115/1.1833366>
- [4] Fakheri, A. (2007). Heat exchanger efficiency. *Journal of Heat Transfer*, 129(9): 1268-1276. <https://doi.org/10.1115/1.2739620>
- [5] Shah, R., Thonon, B., Benforado, D. (2000). Opportunities for heat exchanger applications in environmental systems. *Applied Thermal Engineering*, 20(7): 631-650. [https://doi.org/10.1016/S1359-4311\(99\)00045-9](https://doi.org/10.1016/S1359-4311(99)00045-9)
- [6] Omer, A.M. (2022). Performance, modelling, measurement and simulation of energy efficiency for heat exchanger, refrigeration and air conditioning. In *Innovative Renewable Energy*, Springer, Cham, 157-176. https://doi.org/10.1007/978-3-030-76221-6_23
- [7] Khalaf, A.F., Basem, A., Hussein, H.Q., Jasim, A.K., Hammoodi, K.A., Al-Tajer, A.M., Omer, I., Flayyih, M.A. (2022). Improvement of heat transfer by using porous media, nanofluid, and fins: A review. *International Journal of Heat and Technology*, 40(2): 497-521. <https://doi.org/10.18280/ijht.400218>
- [8] Edreis, E., Petrov, A. (2020). Types of heat exchangers in industry, their advantages and disadvantages, and the study of their parameters. *IOP Conference Series. Materials Science and Engineering*, 963(1): 012027. <https://doi.org/10.1088/1757-899x/963/1/012027>
- [9] Ghalandari, M., Irandoost Shahrestani, M., Maleki, A., Safdari Shadloo, M., El Haj Assad, M. (2021). Applications of intelligent methods in various types of heat exchangers: A review. *Journal of Thermal Analysis and Calorimetry*, 145(4): 1837-1848. <https://doi.org/10.1007/s10973-020-10425-3>
- [10] Thulukkanam, K. (2024). Heat Exchangers. CRC Press, Boca Raton. <https://doi.org/10.1201/9781003352044>
- [11] Omidi, M., Farhadi, M., Jafari, M. (2017). A comprehensive review on double pipe heat exchangers. *Applied Thermal Engineering*, 110: 1075-1090. <https://doi.org/10.1016/j.applthermaleng.2016.09.027>
- [12] Boda, M., Deshetti, S., Gavade, M. (2017). Design and development of parallel-counter flow heat exchanger. *International Journal of Innovative Research in Advanced Engineering*, 4(2): 29-35.
- [13] Cabezas-Gómez, L., Aparecido Navarro, H., Maria Saiz-Jabardo, J. (2007). Thermal performance of multipass parallel and counter-cross-flow heat exchangers. *Journal of Heat Transfer*, 129(3): 282-290. <https://doi.org/10.1115/1.2430719>
- [14] Sridharan, M. (2020). Predicting performance of double-pipe parallel- and counter-flow heat exchanger using fuzzy logic. *Journal of Thermal Science and Engineering Applications*, 12(3): 031006. <https://doi.org/10.1115/1.4044696>
- [15] Malik, A.U., Al-Fozan, S.A., Al-Muaili, F. (2015). Corrosion of heat exchanger in thermal desalination plants and current trends in material selection. *Desalination and Water Treatment*, 55(9): 2515-2525. <https://doi.org/10.1080/19443994.2014.940642>
- [16] Trafczynski, M., Markowski, M., Urbaniec, K. (2023). Energy saving and pollution reduction through optimal scheduling of cleaning actions in a heat exchanger network. *Renewable and Sustainable Energy Reviews*, 173: 113072. <https://doi.org/10.1016/j.rser.2022.113072>
- [17] Klemes, J.J., Arsenyeva, O., Kapustenko, P., Tovazhnyanskyy, L. (2015). Compact Heat Exchangers for Energy Transfer Intensification: Low Grade Heat and Fouling Mitigation. CRC Press.
- [18] Morandin, M., Maréchal, F., Mercangöz, M., Buchter, F. (2012). Conceptual design of a thermo-electrical energy storage system based on heat integration of the thermodynamic cycles – Part A: Methodology and base case. *Energy*, 45(1): 375-385. <https://doi.org/10.1016/j.energy.2012.03.031>
- [19] Xiao, W., Wang, K., Jiang, X., Li, X., Wu, X., Hao, Z., He, G. (2019). Simultaneous optimization strategies for heat exchanger network synthesis and detailed shell-and-tube heat-exchanger design involving phase changes using GA/SA. *Energy*, 183: 1166-1177. <https://doi.org/10.1016/j.energy.2019.06.151>
- [20] Zhang, K., Li, M.J., Liu, H., Xiong, J.G., He, Y.L. (2021). A general and rapid method to evaluate the effect of flow maldistribution on the performance of heat exchangers. *International Journal of Thermal Sciences*, 170: 107152. <https://doi.org/10.1016/j.ijthermalsci.2021.107152>
- [21] Osintsev, K., Aliukov, S., Kuskarbekova, S., Tarasova, T., Karelin, A., Konchakov, V., Kornyakova, O. (2023). Increasing thermal efficiency: Methods, case studies, and integration of heat exchangers with renewable energy sources and heat pumps for desalination. *Energies*, 16(13): 4930. <https://doi.org/10.3390/en16134930>
- [22] Lodhi, S.K., Hussain, H.K., Hussain, I. (2024). Using AI to increase heat exchanger efficiency: An extensive analysis of innovations and uses. *International Journal of Multidisciplinary Sciences and Arts*, 3(4): 1-14. <https://doi.org/10.47709/ijmdsa.v3i4.4617>
- [23] Shipley, M.A., Hampson, A., Hedman, B., Garland, P., Bautista, P. (2008). Combined heat and power: Effective energy solutions for a sustainable future. Oak Ridge National Laboratory.
- [24] Liu, Z.Y., Varbanov, P.S., Klemeš, J.J., Yong, J.Y. (2016). Recent developments in applied thermal engineering: Process integration, heat exchangers, enhanced heat transfer, solar thermal energy, combustion and high temperature processes and thermal process modelling. *Applied Thermal Engineering*, 105: 755-762. <https://doi.org/10.1016/j.applthermaleng.2016.06.183>
- [25] Patel, A. (2023). Heat exchanger materials and coatings: Innovations for improved heat transfer and durability. *International Journal of Engineering Research and Applications (IJERA)*, 13(9): 131-142. <https://doi.org/10.9790/9622-1309131142>

- [26] Kannojiya, V., Gaur, R., Yadav, P., Sharma, R. (2018). Performance investigation of a double pipe heat exchanger under different flow configuration by using experimental and computational technique. *Archive of Mechanical Engineering*, 65(1): 27-41. <https://doi.org/10.24425/ame.2018.123895>
- [27] Koca, T., Citlak, A. (2021). Design and analysis of double-pipe heat exchanger using both helical and rotating inner pipe. *Thermal Science*, 25(2): 1545-1559. <https://doi.org/10.2298/tsci201010066k>
- [28] Sadighi Dizaji, H., Jafarmadar, S., Mobadersani, F. (2015). Experimental studies on heat transfer and pressure drop characteristics for new arrangements of corrugated tubes in a double pipe heat exchanger. *International Journal of Thermal Sciences*, 96: 211-220. <https://doi.org/10.1016/j.ijthermalsci.2015.05.009>
- [29] Gabir, M.M., Alkhafaji, D. (2021). Comprehensive review on double pipe heat exchanger techniques. *Journal of Physics. Conference Series*, 1973(1): 012013. <https://doi.org/10.1088/1742-6596/1973/1/012013>
- [30] Klewicki, J.C. (2010). Reynolds number dependence, scaling, and dynamics of turbulent boundary layers. *Journal of Fluids Engineering*, 132(9): 094001. <https://doi.org/10.1115/1.4002167>
- [31] Lagerstrom, P.A. (1996). *Laminar Flow Theory*. Princeton University Press.
- [32] Pagliarini, G., Barozzi, G.S. (1991). Thermal coupling in laminar flow double-pipe heat exchangers. *Journal of Heat Transfer*, 113(3): 526-534. <https://doi.org/10.1115/1.2910595>
- [33] Schlichting, H., Gersten, K. (2016). *Boundary-Layer Theory*. Springer.
- [34] Gad-el-Hak, M., Bandyopadhyay, P.R. (1994). Reynolds number effects in wall-bounded turbulent flows. *Applied Mechanics Reviews*, 47(8): 307-365. <https://doi.org/10.1115/1.3111083>
- [35] Terekhov, V.I. (2021). Heat transfer in highly turbulent separated flows: A review. *Energies*, 14(4): 1005. <https://doi.org/10.3390/en14041005>
- [36] Mohamed, H.A., Negeed, E.S.R., Alhazmy, M.M. (2022). Experimental investigation of increasing heat transfers inside a double pipe heat exchanger by using Al₂O₃ nanofluid. *Journal of Engineering Sciences and Information Technology*, 6(3): 107-123. <https://doi.org/10.26389/ajsrp.f201221>
- [37] Majeed, N.H., Mushatet, K.S. (2025). Simulation of turbulent flow and heat transfer in A double tube heat exchanger with twisted tape. *University of Thi-Qar Journal for Engineering Sciences*, 15(1): 107-119. <https://doi.org/10.31663/utjes.15.1.680>
- [38] Dimotakis, P.E. (2000). The mixing transition in turbulent flows. *Journal of Fluid Mechanics*, 409: 69-98. <https://doi.org/10.1017/s0022112099007946>
- [39] Rao, R.V., Saroj, A., Ocloń, P., Taler, J. (2020). Design optimization of heat exchangers with advanced optimization techniques: A review. *Archives of Computational Methods in Engineering: State of the Art Reviews*, 27(2): 517-548. <https://doi.org/10.1007/s11831-019-09318-y>
- [40] Guo, Z.Y., Liu, X.B., Tao, W.Q., Shah, R.K. (2010). Effectiveness-thermal resistance method for heat exchanger design and analysis. *International Journal of Heat and Mass Transfer*, 53(13-14): 2877-2884. <https://doi.org/10.1016/j.ijheatmasstransfer.2010.02.008>
- [41] Pordanjani, A.H., Aghakhani, S., Afrand, M., Mahmoudi, B., Mahian, O., Wongwises, S. (2019). An updated review on application of nanofluids in heat exchangers for saving energy. *Energy Conversion and Management*, 198: 111886. <https://doi.org/10.1016/j.enconman.2019.111886>
- [42] Nagarani, N., Mayilsamy, K., Murugesan, A., Kumar, G.S. (2013). Review of utilization of extended surfaces in heat transfer problems. *Renewable and Sustainable Energy Reviews*, 29: 604-613. <https://doi.org/10.1016/j.rser.2013.08.068>
- [43] Choi, T.J., Park, M.S., Kim, S.H., Jang, S.P. (2021). Experimental study on the effect of nanoparticle migration on the convective heat transfer coefficient of EG/Water-based AL₂O₃ nanofluids. *International Journal of Heat and Mass Transfer*, 169: 120903. <https://doi.org/10.1016/j.ijheatmasstransfer.2021.120903>
- [44] Bashirmezhad, K., Bazri, S., Safaei, M.R., Goodarzi, M., Dahari, M., Mahian, O., Dalkılıç, A.S., Wongwises, S. (2016). Viscosity of nanofluids: A review of recent experimental studies. *International Communications in Heat and Mass Transfer*, 73: 114-123. <https://doi.org/10.1016/j.icheatmasstransfer.2016.02.005>
- [45] Sivalakshmi, S., Raja, M., Gowtham, G. (2020). Effect of helical fins on the performance of a double pipe heat exchanger. *Materials Today Proceedings*, 43: 1128-1131. <https://doi.org/10.1016/j.matpr.2020.08.563>
- [46] Siddique, M., Khaled, A.A., Abdulhafiz, N.I., Boukhary, A.Y. (2010). Recent Advances in heat transfer Enhancements: A review report. *International Journal of Chemical Engineering*, 2010: 1-28. <https://doi.org/10.1155/2010/106461>
- [47] Bhutta, M.M.A., Hayat, N., Bashir, M.H., Khan, A.R., Ahmad, K.N., Khan, S. (2011). CFD applications in various heat exchangers design: A review. *Applied Thermal Engineering*, 32: 1-12. <https://doi.org/10.1016/j.applthermaleng.2011.09.001>
- [48] Norton, T., Tiwari, B., Sun, D. (2012). Computational fluid dynamics in the design and analysis of thermal Processes: A review of recent advances. *Critical Reviews in Food Science and Nutrition*, 53(3): 251-275. <https://doi.org/10.1080/10408398.2010.518256>
- [49] Kotian, S., Methekar, N., Jain, N., Naik, P. (2020). Heat transfer and fluid flow in a double pipe heat exchanger, part I: Experimental investigation. *Asian Review of Mechanical Engineering*, 9(2): 7-15. <https://doi.org/10.51983/arme-2020.9.2.2482>
- [50] Banu, P.S.A., Azhar, M., Mahbubul, I.M., Raj, A.G.S. (2024). Simulation and validation of phase change heat exchangers. *Energy and Thermofluids Engineering*, 4: 1-10. <https://doi.org/10.38208/ete.v4.709>
- [51] Debtera, B., Neme, I., Prabhu, V. (2018). CFD simulation of a double pipe heat exchanger: Analysis conduction and convection heat transfer. *International Journal of Scientific Research and Review*, 7: 12.
- [52] Hasan, H.M., Abdulmajeed, B.A. (2023). The evaluation of the performance of the heat exchanger of a triple concentric tube configuration with ionic liquid (imidazolium) and MWCNT ionanofluid. *Journal of Thermal Engineering*, 9(6): 1452-1465. <https://doi.org/10.18186/thermal.1396700>
- [53] Almehaal, M.A., Choubani, K. (2023). Using the log

mean temperature difference (LMTD) and E-NTU methods to analyze heat and mass transfer in direct contact membrane distillation. *Membranes*, 13(6): 588. <https://doi.org/10.3390/membranes13060588>

$T_{h,1}, T_{h,2}$ inner and outer hot temperatures, K
 $T_{c,1}, T_{c,2}$ inner and outer cold temperatures, K

Greek symbols

Re Reynolds number
 ρ fluid density, Kg/m³
u fluid velocity, m/s
 D_h hydraulic diameter, m
 μ dynamic viscosity of fluid, N·s/m²
 ΔP pressure drop, pa
 f friction loss

NOMENCLATURE

HE heat exchanger
 ΔT_{LM} (LMTD) log mean temperature difference, K
CFD computational fluid dynamics
Q heat transfer rate, Watt
A area, m²
U overall heat transfer coefficient, W/m²·K